Appl Nanosci (2014) 4:37–46
DOI 10.1007/s13204-012-0181-x

ORIGINAL ARTICLE

A simple degradation method for sulfur mustard at ambient conditions using nickelphthalocyanine incorporated polypyrrole modified electrode

Pushpendra K. Sharma · Bhavna Sikarwar · Garima Gupta · Anil K. Nigam · Brijesh K. Tripathi · Pratibha Pandey · Mannan Boopathi · Kumaran Ganesan · Beer Singh

Received: 30 August 2012 / Accepted: 26 November 2012 / Published online: 11 December 2012
© The Author(s) 2012. This article is published with open access at Springerlink.com

Abstract Electrocatalytic degradation of sulfur mustard (SM) was studied using a gold electrode modified with nickelphthalocyanine and polypyrrole (NiPc/pPy/Au) in the presence of a cationic surfactant cetyltrimethyl ammonium bromide. Several techniques such as cyclic voltammetry, scanning electron microscopy, electrochemical impedance spectroscopy, energy dispersive X-ray spectroscopy and Raman spectroscopy have been employed for the characterization of modified electrodes. NiPc/pPy/Au modified electrode exhibited excellent electrochemical sensing and degradation ability towards SM. The present modification indicated two electron involvements in the electrocatalytic degradation of SM in addition to being an irreversible adsorption controlled process. Degraded products were identified by gas chromatography-mass spectrometry. Moreover, electrochemical parameters of oxidation of SM such as heterogeneous rate constant (0.436 s^{-1}), transfer coefficient (0.47) and the number of electrons involved (2) were deduced from cyclic voltammetry results. The NiPc/pPy/Au modified electrode showed excellent electrocatalytic degradation towards SM when compared to bare gold, pPy/Au and NiPc/Au modified electrode at ambient conditions.

Keywords Chemical warfare agents · Electrocatalysis · Nickelphthalocyanine · Sulfur mustard

P. K. Sharma · B. Sikarwar · G. Gupta · A. K. Nigam · B. K. Tripathi · P. Pandey · M. Boopathi (✉) · K. Ganesan · B. Singh
Defence Research and Development Establishment, DRDO, Gwalior 474 002, India
e-mail: boopathi@drde.drdo.in

Introduction

The sulfur mustard [Bis(2-chloroethyl) sulphide or SM] is the most terrible chemical warfare agent (CWA) and was employed in the World War I (WWI), named for its distinctive odor, reminiscent of wild mustard or garlic. SM persists in the environment for long periods because of its low volatility and slow rate of decomposition (Watson and Griffin 1992; Sidell et al. 1997). It was the most effective chemical warfare agent used during WWI and this efficiency earned for mustard gas, the sobriquet "King of the Battle Gases" (Okumura et al. 1996; World Health Organization 1970). Although there are presently more toxic chemical warfare agents, mustard gas remained as the chemical weapon of choice in modern strategic warfare and is evidenced by its use during the Iran–Iraq conflict between 1983 and 1988 (United Nations Security Council. Report of the mission dispatched by the Secretary General to investigate allegations of the use of chemical weapons in the conflict between the Islamic Republic of Iran and Iraq. April 25, 1988. S/19823 and S/19823/Addendum 1, 1988). The toxicity of SM as a blistering agent is of much greater importance than its capacity to kill in terms of lethal dose 50 %. In fact, compared with the nerve agents, SM is exhibiting relatively low acute lethal toxicity (Maynard 1995). Among the survivors of mustard gas attacks in WWI and in the Iran–Iraq War, nearly all victims suffered from skin and eye burns and respiratory injuries (Balali-Mood and Navaeian 1986; Fouyn et al. 1991).

The persistence of mustard gas in the environment, however, has made it more difficult to destroy than other CW agents (despite its relatively rapid hydrolysis as indicated by a short half-life of 4–8 min) (Bartlett and Swain 1949); the low solubility in water (only about 900 mg/L) gives rise to its environmental stability. Therefore, SM is

buried in the soil, where it cannot vaporize and can remain stable for years (Munro et al. 1999). Due to above characteristics and the extremely hazardous nature of SM and many related compounds, it has become an urgent task to immediately identify and decompose the stockpiles.

Conducting polymers have been extensively used since last four decades as novel materials for potential applications in various electrochemical devices including actuators (Shoa et al. 2010), chemical and biosensors (Koh et al. 2010), capacitors (Lee et al. 2010) and electrocatalyst (Qu et al. 2010). The most commonly applied polymers for sensing applications have been based on polypyrrole (pPy), polyaniline (PANI), polythiophene (PTP) and their derivatives (Pirsa and Alizade 2010). Among these conducting polymers, pPy has been extensively studied owing to its excellent conductivity, high yield in redox process, gas sensing ability, optimum performance at room temperature, response to a wide range of volatile organic compounds (VOCs) and environmental stability (Pirsa and Alizade 2010; Hamilton et al. 2005; Arora et al. 2006; Planche et al. 1994). Attempts have been made to improve electrocatalytic activity and stability of pPy by doping with metal-phthalocyanines. Phthalocyanines have excellent electrical conducting properties, owing to their high conjugated structure. Hence, several studies appeared in the literature regarding the electrocatalytic redox behavior of organic compounds because of their high conjugated structure, thermal stability, chemical inertness and ready availability (Achar et al. 2003; Karaoglan et al. 2011; Torre et al. 2001; Duarte et al. 2008). The electrocatalytic oxidation of organic compounds readily occurs on bare electrodes; however, oxidation results in the formation of unwanted products which poisons the electrode, thus decreasing the oxidation current (Nyokong et al. 2006). To overcome this problem, modified electrodes particularly, metallophthalocyanine modified electrodes have shown good electrocatalytic activity due to the accessibility of a range of oxidation states centred on the phthalocyanine unit or on the central metal (Lever et al. 1993). Transition-metal phthalocyanine modified electrodes were extensively studied due to their numerous applications in electrocatalysis such as O_2 (Pal and Ganesan 2009; Baker et al. 2008; Mamuru et al. 2010; Zagal et al. 2010; Sun et al. 2011; Arechederra et al. 2010), thiols (Griveau et al. 2004; Sehlotho et al. 2006) and hydrazine oxidation (Paredes-Garcia et al. 2005; Ozoemena and Nyokong 2005).

The present study focused on the electrocatalytic oxidation and degradation of SM. In this investigation nickelphthalocynine (NiPc) incorporated pPy was prepared on the gold electrode surface, for the purpose of increasing stability and electrocatalytic activity of the modification. Surface and functional group of the modified electrodes were characterized using scanning electron microscopy (SEM) and Raman spectroscopy, respectively. Electrochemical and electrocatalytic properties of NiPc/pPy/Au modified electrodes were studied by cyclic voltammetry (CV) and electrochemical impedance spectroscopy (EIS).

Experimental

Chemical and reagents

Surfactant cetyl trimethyl ammonium bromide (CTAB) and sodium perchlorate (Sigma-Aldrich) were used as received. Py (98 % Aldrich) was purified under a reduced pressure and stored in a refrigerator. SM was synthesized in our establishment at declared facility by the trained chemist with appropriate protective measures (Caution: SM is a CWA and care should be taken while using). Nickel (II) phthalocyanine was from Sigma-Aldrich and all other chemicals and reagents used were of AR grade. The pH 6.0 phosphate buffer solution was used in this study for the electrochemical characterization prepared from KH_2PO_4 and K_2HPO_4.

Instruments

CV and EIS experiments were performed using a Potentiostat/Galvanostat with frequency response analyzer (Autolab-302 with FRA-II, The Netherlands). ESEM-EDX (Quanta400-ESEM with EDAX-FEI, The Netherlands), Renishaw Invia Raman Microscope (Gloucestershire, UK) and Eutech instruments pH meter (pH-1500, Singapore) were utilized in this study. Agilent GC (6890 N)–MS system (5973 Inert) was used for the characterization of degradation products. All electrochemical experiments were performed at a temperature of 25 ± 2 °C using a conventional three-electrode system. The gold working, Ag/AgCl (3 M KCl) reference and the auxiliary platinum electrodes used in this study are supplied by M/s Metrohm, Switzerland.

Electrode modification

The gold working electrode was polished carefully with alumina powder (0.05 μm) on a soft polishing cloth (Buehler). After sonicating in absolute ethanol, then in water for 5 min, successively, it was electrochemically treated with cyclic scanning in the potential range from −0.5 to 1.3 V at the scan rate of 50 mV s^{-1} in 0.1 M H_2SO_4 until a stable cyclic voltammogram for a clean Au electrode was obtained. The electrodeposition of NiPc and Py was carried out by cyclic voltammetry method from an aqueous solution containing 0.1 M Py and 0.1 M sodium perchlorate, 0.004 M NiPc and 0.001 M cationic surfactant CTAB in the potential range between −0.2 V and 1.0 V at

the 50 mV s^{-1}. Same potential range and scan rate were used for electrodeposition of the pure Py and pure NiPc in presence of sodium perchlorate and CTAB. When removed from the solution, all the modified gold electrodes were rinsed with distilled water to remove unbound materials from the electrode surface and then dried.

Characterization of the pPy/NiPc/Au, pPy/Au and NiPc/Au modified electrodes

The pPy/NiPc/Au, pPy/Au and NiPc/Au modified electrodes were extensively characterized by CV, EIS and Raman spectroscopy to know the electrochemical activities, interfacial properties and functional groups present on the electrode surface, respectively. Surface morphology and elemental composition of the modified electrodes were characterized by SEM and EDX, respectively.

Results and discussion

Simultaneous electrodeposition of pPy and NiPc in presence of CTAB

It is well known that the NiPc is not soluble in polar solvents and to make it soluble in polar solvents, CTAB surfactant was used (Saji 1988) in this study. NiPc molecules are adsorbed on the surfactant as they have hydrophobic and hydrophilic ends, thereby making the NiPc to dissolve in the aqueous solution. Electrodeposition of Py, NiPc and NiPc/pPy was carried out by CV method as discussed in experimental section.

Characterization of electrode surface by SEM and EDX

The modification of gold electrode with NiPc and pPy was investigated by SEM and EDX to explore surface morphology and elemental composition, respectively. SEM experiments are carried out to know the surface morphologies of the samples such as pPy/Au, NiPc/Au and NiPc/pPy/Au. SEM image shows (Fig. 1a, b) flakes and globular structure for NiPc/Au and pPy/Au, respectively. However, surface morphology of NiPc/pPy/Au sample is exhibiting nano-particles and also agglomerated nano-particles due to incorporation of NiPc with pPy as shown in Fig. 1c.

The energy dispersive X-ray analysis (EDX) is performed to know the elemental composition of NiPc/Au, pPy/Au and NiPc/pPy/Au. The elemental composition is presented as the corresponding spectra in Fig. 2a, b and c for NiPc/Au, pPy/Au and NiPc/pPy/Au, respectively. Figure 2a shows the spot elemental composition of NiPc modified electrode which reveals the presence of carbon, nitrogen, oxygen, potassium and nickel.

Figure 2b shows the EDX spectrum of pPy/Au, this sample contains following elements namely carbon, nitrogen, oxygen, potassium and chlorine which shows electrode surface modified with pPy. The EDX spectrum of NiPc/pPy/Au is shown in Fig. 2c, this sample contains elements namely carbon, nitrogen, oxygen, nickel, chlorine and gold. All these data indicates incorporation of NiPc with pPy. In addition, absence of bromine confirms non inclusion of CTAB into the polymer.

Raman spectroscopic characterization

Raman spectroscopy is a significant technique to know about functional groups in turn on the modified electrode surface. It was also confirmed that Au electrode is modified with NiPc and pPy. A typical Raman spectrum of the NiPc in the region of 200–2,000 cm^{-1} is given in Fig. 3a. Peak positions of all the observed bands are comparable with the earlier results on other metalphthalocyanines (Li et al. 1992; Souto et al. 1991; Aroca et al. 1990). The bands at 596, 687 and 1,307 cm^{-1} are due, respectively, to benzene ring deformation, macrocycle breathing and pyrrole ring stretching vibrations (Aroca et al. 1990). The highest-intensity band at 1,549 cm^{-1} is very close to the reported values of C=N (aza), C=C (pyrrole), C=C (benzene) ring stretching vibrations (Aroca et al. 1990).

Nevertheless, in recent studies it has been confirmed by an isotopic substitution of N that the band at 1,549 cm^{-1} is mainly due to C=N aza group stretching (ν_{C-N}) vibration. Other weaker features at 962 and 1,012 cm^{-1}; 1,341 and 1,456 cm^{-1} are attributed to C–H deformation, isoindole ring stretching and C–N pyrrole stretching vibrations, respectively. The medium strong bands at 280 and 687, and 1,142 cm^{-1} are mainly due to isoindole ring deformation, macrocycle deformation, and pyrrole ring breathing vibrations, in that order. But after polymerization of the NiPc Peak positions of most important groups, observed bands of the isoindole ring stretching, C–N pyrrole stretching and C=N (aza) ring stretching are shifted towards a high wave number as shown in Table 1 and Fig. 3b.

However, Raman spectrum of the polypyrrole modified gold electrode (Liu 2002) is shown in Fig. 3c. The strongest peak for pPy backbone stretching is located at 1,594 cm^{-1}. The broad peak at 1,230–1,487 cm^{-1} corresponds to the C–H and N–H in-plane bending vibration. In addition, the broad peak at 1,051–1,087 cm^{-1} is due to C–H and N–H out of plane bending vibration. The peak at 934 cm^{-1} is attributed to C–C ring stretching and C–H in-plane bending vibration. But after incorporation of NiPc in pPy, two extra peaks at 618 and 685 cm^{-1} are observed due to benzene ring deformation and macrocycle breathing, respectively. Moreover, peak positions of the most

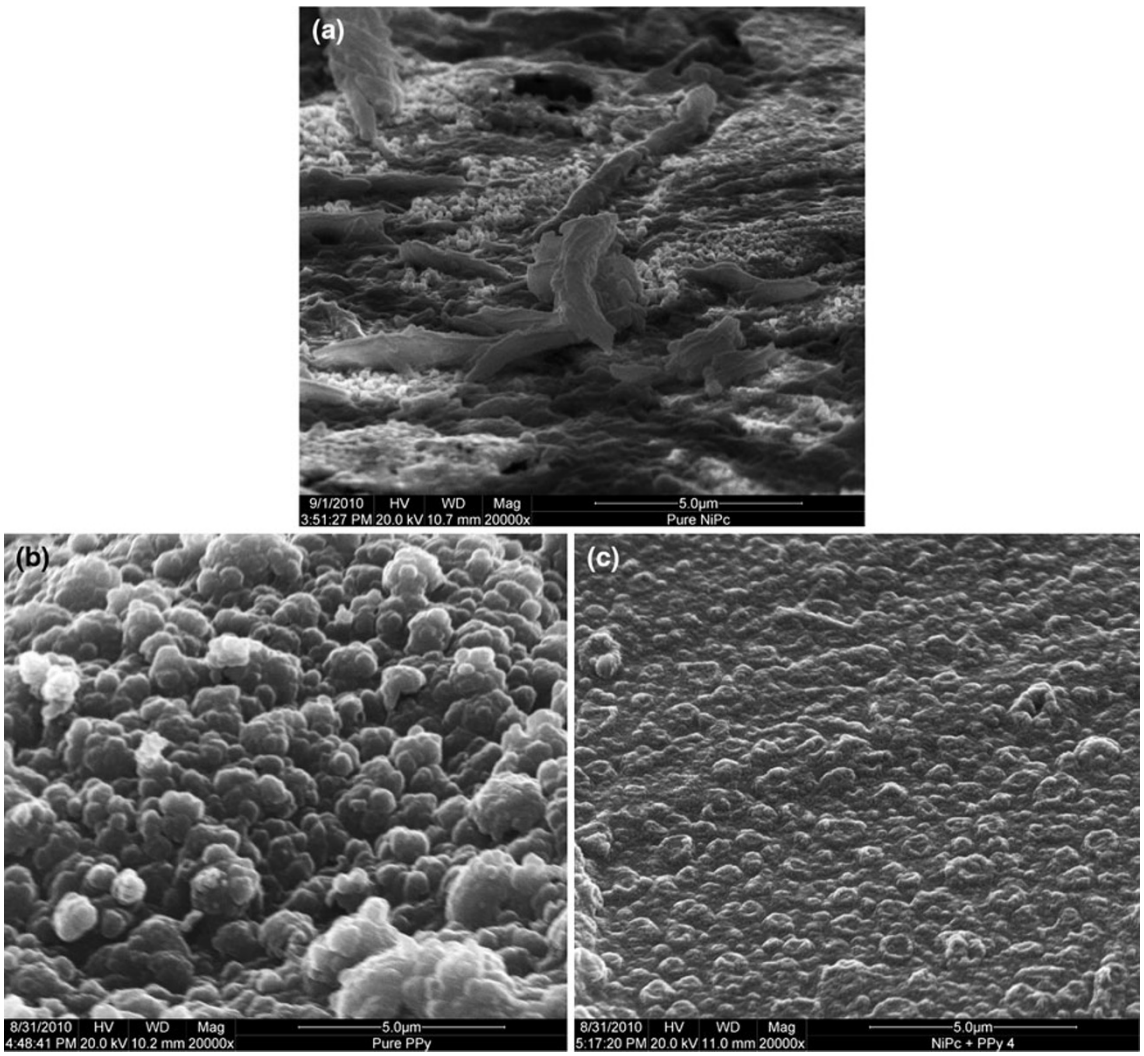

Fig. 1 SEM images for deposition of **a** NiPc, **b** pPy and **c** NiPc/pPy on the Au electrode

important groups observed bands are shifted towards a higher wave number is known to show a remarkable sensitivity to the metal ion present and provides a specific signature for phthalocyanine studied (Zhang et al. 2004; Tackley et al. 2001) as shown in Fig. 3d.

Electrochemical studies of SM

EIS is a powerful and sensitive characterization tool for studying the charge transfer processes occurring at electrode/solution or modified electrode/solution interfaces. The impedance analysis was carried out under the oscillation potential 0.01 V from 10,000 to 0.1 Hz at open circuit potential. The Nyquist plot was fitted and analysed using the Randles equivalent circuit [Fig. 4a (insert)], which takes into consideration the diffusion and kinetic control parameters (Westbroek et al. 2005; Kumar and Lakshminarayanan 2007; Yang and Li 2005). The Randles equivalent circuit used for fitting impedance data consisted of the solution resistance (R_s) connected in series to the parallel combination of the capacitance (C_{dl}) and charge transfer resistance (R_{ct}) in series with Warburg impedance (Z_w). The R_s values (Table 2) between bare and the different modifications on Au electrodes were not significantly different (0.406–0.466 kΩ).

The polymers on the electrode surfaces are not expected to change the solution resistance significantly, hence this was expected. The C_{dl} values (Table 2) were different with bare Au, NiPc/pPy/Au without SM and NiPc/pPy/Au with SM electrodes showing the value of 0.920, 1.427 and 0.482 μF, respectively. Warburg impedance is also different for different modified electrodes and the value found to be 0.8343×10^{-5}, 0.4235×10^{-4} and 0.3015×10^{-5}, respectively for bare Au, NiPc/pPy/Au without SM and NiPc/pPy/Au with SM electrodes. The differences show the different conducting abilities of the different modified electrodes.

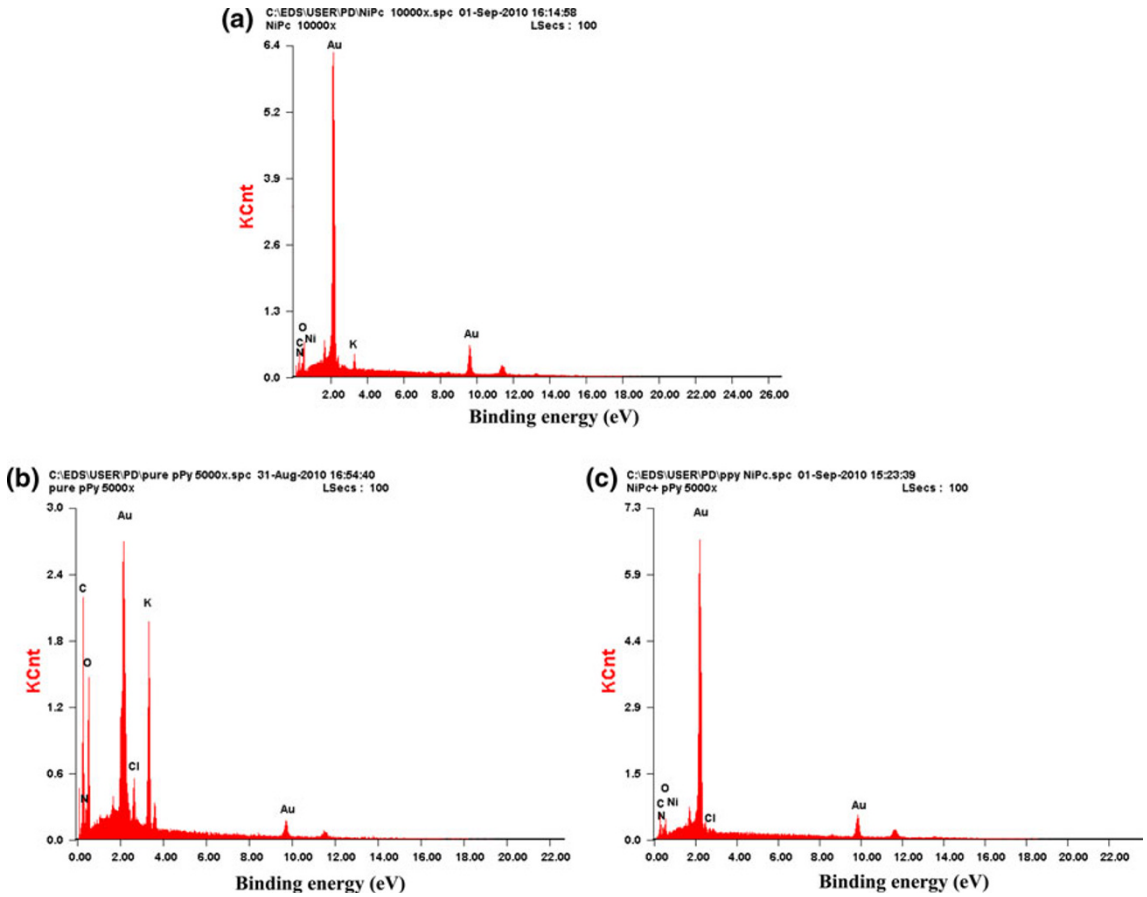

Fig. 2 EDX for **a** NiPc, **b** pPy and **c** NiPc/pPy on the Au electrode

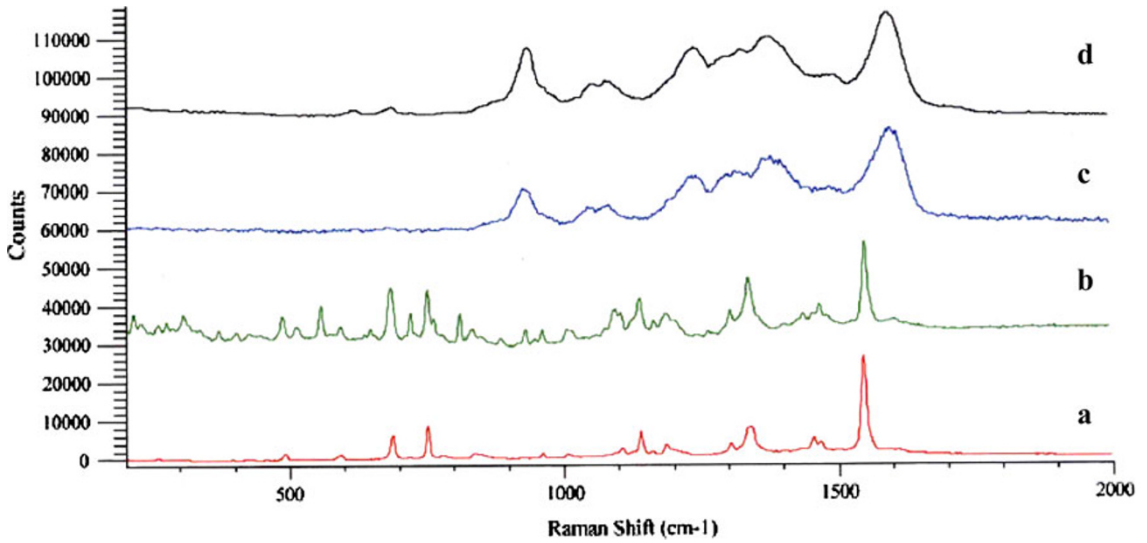

Fig. 3 Raman spectra for **a** NiPc powder, **b** NiPc modified electrode, **c** pPy modified electrode and **d** NiPc/pPy modified electrode

Figure 4a shows the impedance spectra of bare Au electrode in phosphate buffer (pH 6.0) solution with charge transfer resistance (R_{ct}) value 113.3 kΩ. The Nyquist plots recorded in the presence of the NiPc/pPy/Au as shown in Fig. 4b a semicircle for charge transfer resistance (R_{ct}) 95.0 kΩ are observed. The decreasing charge-transfer resistance for the NiPc/pPy/Au is because of the NiPc/pPy can act as an electron-transfer medium and this enhanced

Table 1 Raman spectroscopy characterization data

Assignment	NiPc powder (cm^{-1})	NiPc/Au (cm^{-1})	pPy/Au (cm^{-1})	NiPc/pPy/Au (cm^{-1})
Isoindole ring deformation	280	304	–	–
Benzene ring deformation	596	596	–	618
Macrocycle breathing	687	684	–	685
Macrocycle deformation	752 and 836	752 and 836	–	–
C–C and C–H in-plane bending vibration	–	–	928	934
C–H deformation	962 and 1,012	962 and 1,013	–	–
C–H and N–H out of plane bending vibration	–	–	1,045 and 1,080	1,051 and 1,087
Pyrrole ring breathing vibration	1,142	1,139	–	–
Pyrrole ring stretching vibration	1,307	1,305	–	–
C–H and N–H in-plane bending	–	–	1230, 1304, 1387 and 1487	1,235, 1,326, 1,388 and 1,496
Isoindole ring stretching	1,341	1,338	–	–
C–N pyrrole stretching vibrations	1,456	1,467	–	–
C=N (aza), C=C (pyrrole), C=C (benzene) ring stretching	1,549	1,551	–	–
C=C (pyrrole) ring stretching	–	–	1,594	1,596

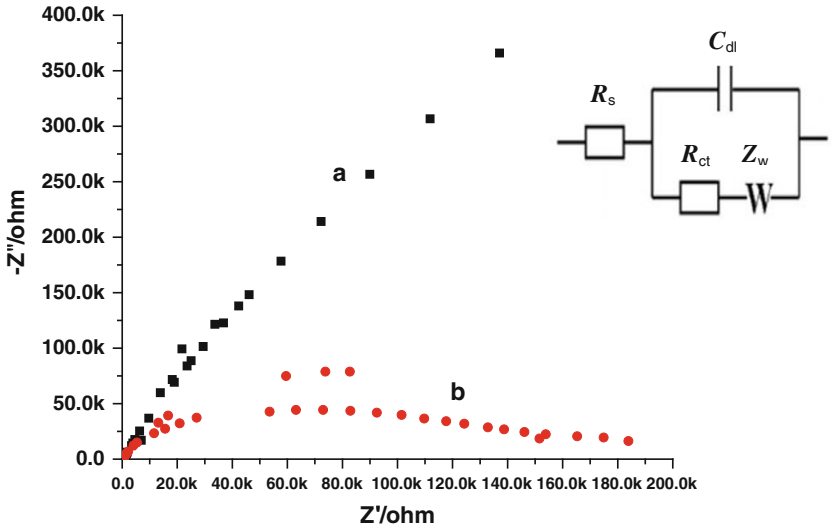

Fig. 4 Electrochemical impedance spectrum of **a** gold electrode and **b** NiPc/pPy/Au modified electrode

Table 2 Electrochemical impedance spectrum characterization data

Electrodes	R_s (kΩ)	R_{ct} (kΩ)	C_{dl} (μF)	Z_w
Bare Au electrode	0.406	113.3	1.427	0.8343×10^{-5}
Modified NiPc/pPy/Au + Blank	0.466	95.0	0.920	0.4235×10^{-4}
Modified NiPc/pPy/Au + SM	0.447	105.5	0.482	0.3015×10^{-5}

electron-transfer rate is attributed to the attachment of NiPc/pPy on Au surface. After adding SM, as shown in Fig. 5b the R_{ct} value increased to 105.0 kΩ from 95.0 kΩ when compared to without SM indicating an increase in charge transfer resistance due to the interaction between NiPc/pPy/Au and SM.

Electrocatalytic oxidation of SM

Figure 6 shows the cyclic voltammograms recorded in pH 6.0 phosphate buffer on bare gold electrode (Fig. 6Aa, Ab without and with SM, respectively), but no peak is observed for SM with this electrode. However, in case of

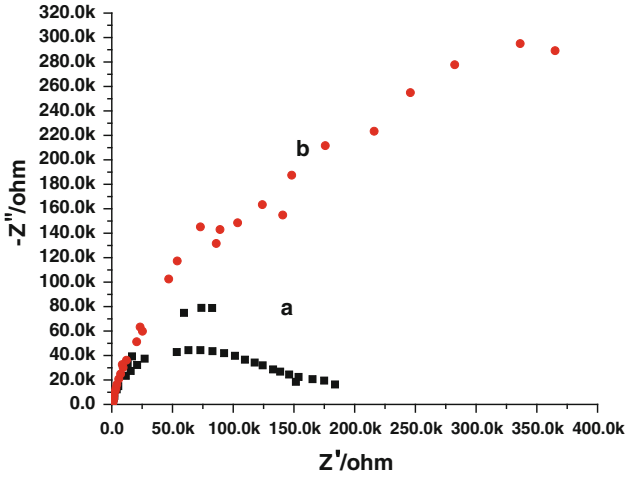

Fig. 5 Electrochemical impedance spectrum of **a** NiPc/pPy/Au modified electrode without SM and **b** NiPc/pPy/Au modified electrode with SM

pPy/Au modified (Fig. 6Ac, Ad without and with SM, respectively) small peak is observed at 1.1 V, but current is very less (5.2 μA) when compared with the NiPc/pPy/Au modified electrode (63.3 μA). Moreover, NiPc/pPy/Au modified electrode (Fig. 6Ae, Af without and with SM, respectively) showed good electrocatalytic activity and distinguish peak at 1.1 V due to oxidation of SM. To investigate the electrocatalytic activity of the NiPc/pPy/Au electrode, concentration variation studies were carried out with SM concentration varying from 3.9×10^{-4} M to 19.5×10^{-4} M (Fig. 6Ba–Be). It is observed from the figures that oxidation peak current is greatly enhanced in the presence of SM with NiPc/pPy/Au electrode and also with increase in the concentration of SM suggesting the involvement of a typical electrocatalytic process in SM oxidation.

To know the nature of electrochemical oxidation process of SM with NiPc/pPy/Au electrode, scan rate variation

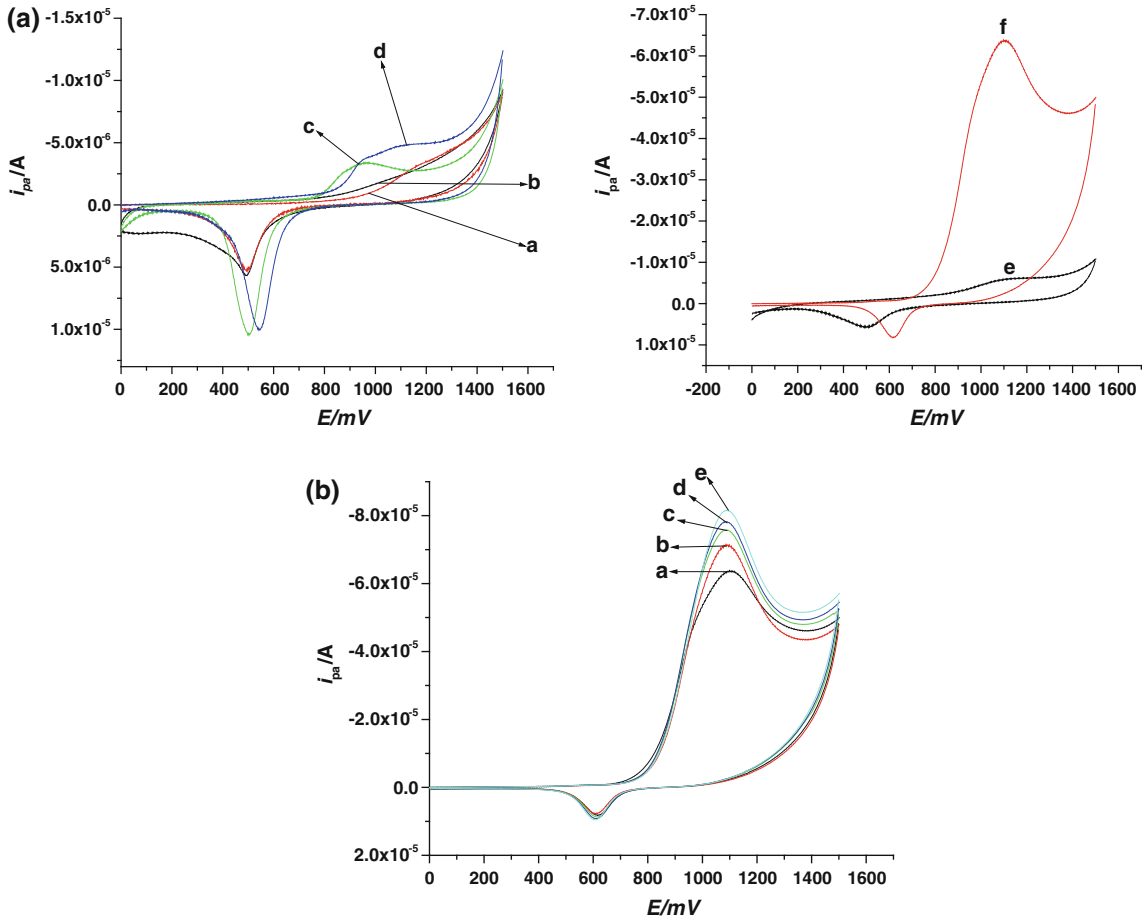

Fig. 6 CVs for (**Aa**, **Ab**) Au electrode without SM and with SM, respectively, (**Ac**, **Ad**) pPy/Au modified electrode without SM and with SM, respectively, (**Ae**, **Af**) NiPc/pPy/Au modified electrode without SM and with SM, respectively, and concentration variation (**Ba–Be**) from 3.9×10^{-4} M to 19.5×10^{-4} M

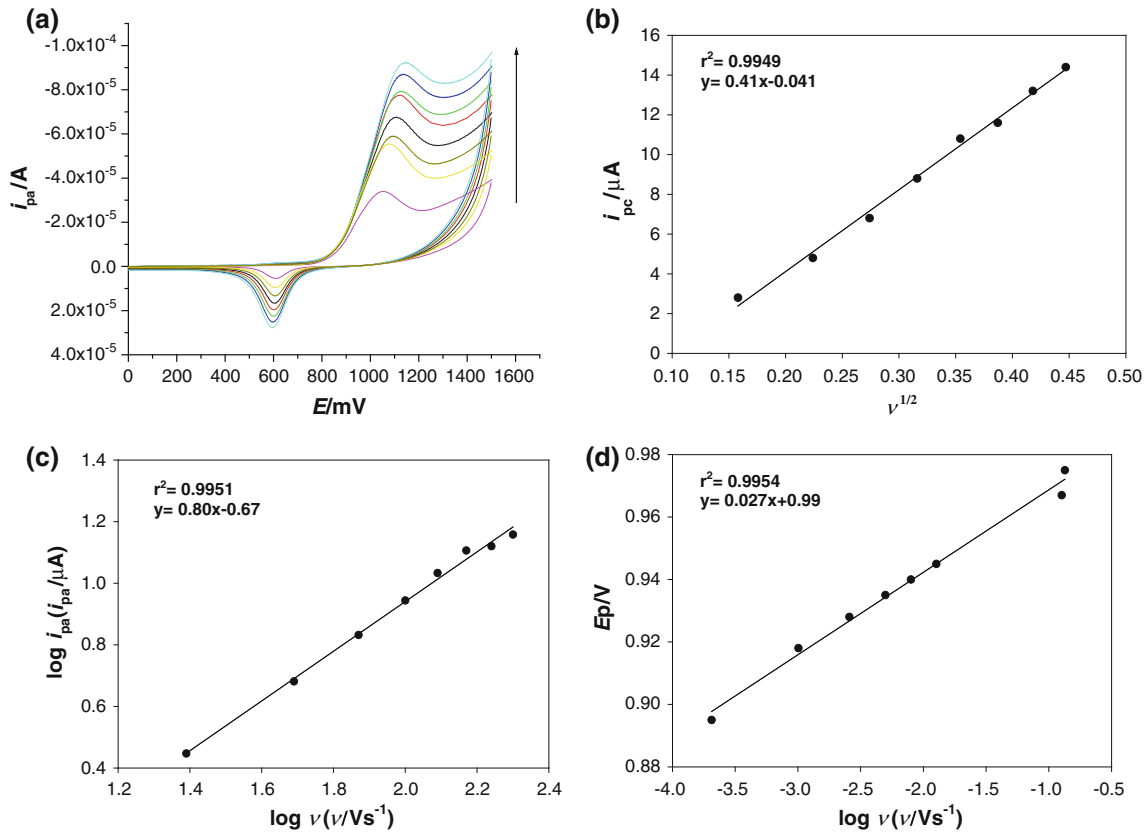

Fig. 7 **a** Effect of scan rate on SM oxidation in pH 6.0 phosphate buffer solution (scan rate: 25–200 mV/s with 25 mV/s increment), **b** plot of anodic peak current (i_{pa}) vs. root scan rate ($v^{1/2}$), **c** plot of log of anodic peak current (i_{pa}) vs. log v and **d** plot of anodic peak potential (E_p) vs. ln v

studies were carried out from 25 to 200 mV/s with an increment of 25 mV/s. The resultant CVs are shown in Fig. 7a and an increase in peak current was observed as scan rate was increased with all the peaks observed in forward scan. The scan rate variation studies (Fig. 7b) were conducted with SM in phosphate buffer solution. To further confirm the SM oxidation peak, log i_{pa} and log v graph was plotted (Fig. 7c) and the slope value was found to be 0.80. This confirms the involvement of an adsorption controlled process during the SM oxidation (Greef et al. 1985).

The plot of E_p versus ln v is exhibiting linear relationship as shown in Fig. 7d for the potential scan rate ranging from 25 to 200 mV/s, with the following linear equation $E_p = 0.027 \ln v + 0.99$ ($r^2 = 0.9954$), which confirms that the electrochemical oxidation of SM is a irreversible process. According to Laviron theory (Laviron 1979a) for an irreversible anodic reaction, the relationship between E_p and v is described as follows:

$$E_p = E^0 - RT/(\alpha nF)\{\ln[(RTk_s)/(\alpha nF)] + \ln v\} \quad (1)$$

where E^0 is the formal standard potential, α is the charge transfer coefficient, n is the number of electrons involved in the oxidation of SM, F is the Faraday constant (96,485 C/mol), k_s is the heterogeneous reaction rate constant, R is the universal gas constant and T is the temperature. According to the slope of the straight line of E_p against ln v, the product of α and n was calculated as 0.0474 and 1.30, respectively. The value of E^0 was estimated to be 0.872 V from the intercept of E_p vs. v plot on the coordinate by extrapolating to $v = 0$. Moreover, the value of heterogeneous rate constant (k_s) was calculated from the intercept of the straight line of E_p vs. ln v and it is found to be 0.436 s^{-1}. On the other hand, for an irreversible adsorption controlled process, according to Laviron's theory (Laviron 1979b) a linear relationship between the peak currents and the scan rate is described as follows:

$$i_{pa} = nFA\Gamma v/4RT = nFQv/4RT \quad (2)$$

where i_{pa} is expressed in the unit of ampere, Q (coulomb) is the peak area of voltammogram, by substituting the respective value in Eq. 2, and the number of electrons involved in the anodic oxidation of SM were found to be 1.30. This result suggests that the reduction of SM is approximately as two electron transfer reaction. Therefore the value of α is 0.474.

Identification of degraded products of SM

To see the in situ electrocatalytic degradation capability of NiPc/pPy/Au Au electrode degradation study is performed with SM in phosphate buffer solution. The degradation study of SM was performed by holding the potential at 1.1 V for 10 h. GC–MS data were obtained after silylating the extracted reaction mixture using bis(trimethylsilyl) trifluoro acetamide and the results indicate degraded products of SM, i.e., chloro ethyl ethyl sulphoxide (*m/z* at 63, 78, 12, 140), vinyl ethyl sulphoxide (*m/z* at 47, 59, 76, 104), divinyl sulphone (*m/z* at 27, 47, 75) and diethyl sulphone (*m/z* at 29, 66, 94, 122).

Conclusions

In this work, NiPc was incorporated into pPy in the presence of a cationic surfactant CTAB modified Au electrode using CV during the polymerization of pyrrole in aqueous solution. Surface morphology, elemental composition and functional groups of the modified electrode were characterized using SEM, EDX and Raman spectroscopy, respectively. CV, EIS, SEM and EDX results revealed the presence of NiPc/pPy cover on the electrode surface. These modified electrodes were used to study the electrocatalytic oxidation and degradation of SM. The NiPc/pPy/Au modified electrode showed excellent stability and electrocatalytic activity towards the oxidation of SM than the bare Au and pPy/Au electrodes. This modification can be used for the electrochemical degradation of SM and other CW agents at ambient conditions.

Acknowledgments The authors thank Prof. Dr. M. P. Kaushik, Director, Defence Research and Development Establishment, DRDO, Gwalior 474002 (India) for his keen interest and encouragement.

Open Access This article is distributed under the terms of the Creative Commons Attribution License which permits any use, distribution, and reproduction in any medium, provided the original author(s) and the source are credited.

References

Achar BN, Fohlen GM, Lokesh KS (2003) Degradation study on the thermally stable nickel phthalocyanine sheet polymer. Polym Degrad Stab 80:427–433

Arechederra RL, Artyushkova K, Atanassov P, Minteer SD (2010) Growth of phthalocyanine doped and undoped nanotube using mild synthesis condition for development of noval oxygen reduction catalysis. Appl Mater Interfaces 2:3295–3302

Aroca R, Zeng ZQ, Mink J (1990) Vibrational assignment of totally symmetric modes in phthalocyanine molecules. J Phys Chem Solids 51:135–139

Arora K, Chaubey A, Singhal R, Singh RP, Pandey MK, Samanta SB, Malhotra BD, Chand S (2006) Application of electrochemically prepared polypyrrole–polyvinyl sulphonate films to DNA biosensor. Biosens Bioelectron 21:1777–1783

Baker R, Wilkinson DP, Zhan J (2008) Electrocatalytic activity and stability of substituted iron phthalocyanines towards oxygenreduction evaluated at different temperatures. Electrochim Acta 53:6906–6919

Balali-Mood M, Navaeian A (1986) Clinical and paraclinical findings in 233 patients with sulfur mustard poisoning. In: Heyndrickx A (ed) Proceedings of the Second World Congress on new compounds in biological and chemical warfare. Rijksuniversiteit, Ghent

Bartlett PD, Swain CG (1949) Kinetics of hydrolysis and displacement reactions of β, β′-dichlorodiethyl sulfide (mustard gas) and of β-chloro-β″-hydroxydiethyl sulfide (mustard chlorohydrin). J Am Chem Soc 71:1406–1415

Duarte JC, Luz RCS, Damos FS, Tanaka AA, Kubota LT (2008) A highly sensitive amperometric sensor for oxygen based on iron(II) tetrasulfonated phthalocyanine and iron(III) tetra-(N-methyl-pyridyl)-porphyrin multilayers. Ana Chimica Acta 612:29–36

Fouyn TH, Lison D, Wouters M, Maynard RL, Meredith TJ, Marrs TC, Vale JA, Willems JL, De Leenheer AP, De Bisschop HC (1991) Management of chemical warfare injuries. Lancet 337:121–122

Greef R, Peat R, Peter LM, Pletcher D, Robinson J (1985) Instrumental methods in electrochemistry. Ellis Horwood, Chichester, UK

Griveau S, Gulppi M, Bedioui F, Zagal JH (2004) Electropolymerized cobalt macrocomplex-based films for thiols electro-oxidation: effect of the film formation conditions and the nature of the macrocyclic ligand. Solid State Ionics 169:59–63

Hamilton S, Hepher MJ, Sommervill J (2005) Polypyrrole materials for detection and discrimination of volatile organic compound. Sens Actuators, B 107:424–432

Karaoglan GK, Gumrukcu G, Koca A, Gul A (2011) The synthesis, characterization, electrochemical and spectroelectrochemical properties of a novel, cationic, water-soluble Zn phthalocyanine with extended conjugation. Dyes Pigm 88:247–256

Koh WCA, Son JI, Choe ES, Shim YB (2010) Electrochemical detection of peroxynitrite using a biosensor based on a conducting polymer-manganese ion complex. Anal Chem 82:10075–10082

Kumar PS, Lakshminarayanan V (2007) Electron-transfer studies in a lyotropic columnar hexagonal liquid crystalline medium. Langmuir 23:1548–1554

Laviron E (1979a) General expression of the linear potential sweep voltammogram in the case of diffusionless electrochemical systems. Electroanal Chem 101:19–28

Laviron E (1979b) The use of linear potential sweep voltammetry and of a.c. voltammetry for the study of the surface electrochemical reaction of strongly adsorbed systems and of redox modified electrodes. J Electroanal Chem 100:263–270

Lee H, Cho MS, Kim IH, Nam JD, Lee Y (2010) RuOx/polypyrrole nanocomposite electrode for electrochemical capacitor. Synth Met 160:1055–1059

Lever ABP, Milaeva ER, Speier G (1993) In: Leznoff CC, Lever ABP (eds) Phthalocyanines: properties and applications. VCH Publishers, New York

Li XY, Kim M, Nie S, Carey P, Yu NJ, Zgierski MZ, Limbach HH (1992) In: Kiefer W, Cardona M, Schoack G, Schneider FW, Schrotter HW (eds) Proceedings of international conference on Raman spectroscopy XIII. Wiley, New York

Liu YC (2002) Evidence of chemical effect on surface-enhanced Raman scattering of polypyrrole films electrodeposited on roughened gold substrates. Langmuir 18:174–181

Mamuru SA, Ozoemena KI, Fukuda T, Kobayashi N, Nyokong T (2010) Studies on the heterogeneous electron transport and oxygen reduction reaction at metal (Co, Fe) octabutylsulphonylphthalocyanines supported on multi-walled carbon nanotube modified graphite electrode. Electrochim Acta 55:6367–6375

Maynard RL (1995) Chemical warfare agents. In: Ballantyne B, Marrs T, Turner P (eds) General and Applied Toxicology. MacMillan, London, UK

Munro NB, Talmage SS, Griffin GD, Waters LC, Watson AP, King JF, Hauschild V (1999) The sources, fate, and toxicity of chemical warfare agent degradation products. Environ Health Perspect 107:933–974

Nyokong T, Zagal JH, Bedioui F, Dodelet JP (2006) N4-Macrocyclic metal complexes. Springer, New York

Okumura T, Takasu N, Ishimatsu S, Miyanoki S, Mitsuhashi A, Kumada K, Tanaka K, Hinohara S (1996) Report on 640 victims of the Tokyo subway sarin attack. Ann Emerg Med 28:129–135

Ozoemena KI, Nyokong T (2005) Electrocatalytic oxidation and detection of hydrazine at gold electrode modified with iron phthalocyanine complex linked to mercaptopyridine self-assembled monolayer. Talanta 67:162–168

Pal M, Ganesan V (2009) Zinc phthalocyanine and silver/gold nanoparticles incorporated MCM-41 type materials as electrode modifiers. Langmuir 25:13264–13272

Paredes-Garcia V, Cardenas-Jiron GI, Venegas-Yazigi D, Zagal JH, Paez M, Costamagna J (2005) Through-space and through-bond mixed charge transfer mechanisms on the hydrazine oxidation by cobalt (II) phthalocyanine in the gas phase. J Phys Chem A 109:1196–1204

Pirsa S, Alizade N (2010) Design and fabrication of gas sensor based on nanostructure conductive polypyrrole for determination of volatile organic solvent. Sens Actuators, B 147:461–466

Planche MF, Thieblemont JC, Mazars N, Bidan G (1994) Kinetic study of pyrrole polymerization with iron (III) chloride in water. J Appl Polym Sci 52:1867–1877

Qu B, Xu Y, Deng Y, Peng X, Chen J, Dai L (2010) Polyaniline/carbon black composite as Pt electrocatalyst supports for methanol oxidation: synthesis and characterization. J Appl Polym Sci 118:2034–2042

Saji T (1988) Electrochemical formation of a phthalocyanine thin film by dispersion of micellar aggregates. Chem Lett 17:693–696

Sehlotho N, Nyokong T, Zagal JH, Bedioui F (2006) Electrocatalysis of oxidation of 2-mercaptoethanol, L-cysteine and reduced glutathione by adsorbed and electrodeposited cobalt tetra phenoxypyrrole and tetra ethoxythiophene substituted phthalocyanines. Electrochim Acta 51:5125–5130

Shoa T, Madden JDW, Mirfakhrai T, Alici G, Spinks GM, Wallace GG (2010) Electromechanical coupling in polypyrrole sensors and actuators. Sens Actuators, A 161:127–133

Sidell FR, Urbanetti JS, Smith WJ (1997) Vesicants: medical aspects of chemical and biological warfare. In: Sidell FR, Takafuji ER, Franz DR (eds) Textbook of military medicine. Part I: warfare, weaponry, and the casualty. Office of the Surgeon General, Department of the Army, Walter Reed Army Medical Center, Washington, DC, pp 197–222

Souto J, Aroca R, Desoja JAJ (1991) Surface-enhanced resonance Raman scattering of a NO_2-bisphthalocyanine adduct in Langmuir-Blodgett monolayers. J Raman Spectr 22:787–790

Sun S, Jiang N, Xia D (2011) Density functional theory study of the oxygen reduction reaction on metalloporphyrins and metallophthalocyanines. J Phys Chem C 115:9511–9517

Tackley DR, Dent G, Smith WE (2001) Phthalocyanines: structure and vibrations. Phys Chem Chem Phys 3:1419–1426

Torre G, Nicolau M, Torres T (2001) In: Nahlac HS (ed) Supramolecular photosensitive and electroactive materials. Gulf Professional Publishing Academic Press

United Nations Security Council. Report of the mission dispatched by the Secretary General to investigate allegations of the use of chemical weapons in the conflict between the Islamic Republic of Iran and Iraq. April 25, 1988. S/19823 and S/19823/Addendum 1 (1988) New York. USA, United Nations

Watson AP, Griffin GD (1992) Toxicity of vesicant agents scheduled for destruction by the Chemical Stockpile Disposal Program. Environ Health Perspect 98:259–280

Westbroek P, Priniotakis G, Kiekens P (2005) Analytical electrochemistry in textiles. Woodhead Publishing Limited and CRC Press LLC, Cambridge, England

World Health Organization (1970) Health aspects of chemical and biological weapons. World Health Organization, New York

Yang L, Li Y (2005) AFM and impedance spectroscopy characterization of the immobilization of antibodies on indium–tin oxide electrode through self-assembled monolayer of epoxysilane and their capture of *Escherichia coli* O157:H7. Biosens Bioelectron 20:1407–1416

Zagal JH, Griveau S, Silva JF, Nyokong T, Bedioui F (2010) Metallophthalocyanine-based molecular materials as catalysts for electrochemical reactions. Coordination Chem Rev 254:2755–2791

Zhang X, Zhang Y, Jiang J (2004) Towards clarifying the N-M vibrational nature of metallo-phthalocyanines. Infrared spectrum of phthalocyanine magnesium complex: density functional calculations. Spectrochim Acta A 60:2195–2200